Available online at www.sciencedirect.com
SCIENCE DIRECT®
Journal of Chromatography A, 1077 (2005) 28–36
JOURNAL OF CHROMATOGRAPHY A
www.elsevier.com/locate/chroma

A first principles explanation for the experimentally observed increase in *A*-term band broadening in small domain silica monoliths and other chromatographic supports

Jeroen Billen*, Piotr Gzil, Gino V. Baron, Gert Desmet

Vrije Universiteit Brussel, Department of Chemical Engineering (CHIS-TW), Pleinlaan 2, B-1050 Brussels, Belgium

Received 8 October 2004; accepted 7 April 2005

Abstract

The present computational study illustrates how the existence of a residual lower limit on the variance of the skeleton and through-pore size of monolithic columns can be expected to severely compromise the possibility to prepare well-performing small domain monolithic columns. Adopting rather conservative estimates for the minimal standard deviation on the pore and the skeleton size (0.2 and 0.04 μm, respectively), the presented calculations show that, if such a fixed lower limit on the size variance exists, it will be impossible to decrease the *A*-term band broadening below a given critical value, no matter how small the domain size is made. From a given critical domain size value on, any attempt to further decrease the domain size without being able to co-reduce the size variance can be expected to be counterproductive and leads to an increase instead of to a further decrease of the plate heights.

Keywords: Liquid chromatography; Band broadening; Silica monoliths; Computational fluid dynamics; Packing heterogeneity; Domain size

1. Introduction

When designing a chromatographic system, each possibility to reduce the flow resistance (for example by switching from a packed bed to a monolithic column format [1,2]) or to increase the available pressure gradient [3,4] should preferentially be exploited by decreasing the size of its unit building block (particle size for a packed bed system and domain size [2] for monolithic columns). The accompanying plate height decrease then always results in faster and/or better separations. Smaller plate heights yield larger plate numbers for a given column length or, if a given plate number is to be achieved, smaller plate heights allow to reduce the column length and the accompanying analysis time. Although the other possible approach to benefit from a reduced flow resistance, i.e., maintaining the particle or domain size and increasing the length L of the column, also yields increased plate numbers, this gain is irrevocably obtained at the expense of an increased analysis time. If operated near their optimal velocity, the current generation of large external porosity capillary monolithic columns with for example $d_s = 2$ μm and $d_{dom} = 10$ μm can yield approximately 36,000 plates in 12 min in columns with $L = 45$ cm, whilst only using an inlet pressure of 3 bar [5]. To exploit the unused available pressure capacity, which is typically of the order of 200–400 bar in a commercial LC system, columns with a length of for example 250 cm could be used [6], yielding over 200,000 plates near their u_{opt}. This would then however require roughly 1 h of analysis time. Even columns with a length of 10 m, potentially yielding over one million plates, can be envisioned [7]. This would of course constitute an unprecedented performance, but many applications in LC do not require this large number of theoretical plates, and are certainly not served by the increased analysis time (roughly 10–20 h for the 10 m column). A much broader and economically more relevant field of application would be opened if the high porosity columns used in [5] could be prepared with a smaller domain and skeleton

* Corresponding author. Tel.: +32 2 629 36 17; fax: +32 2 629 32 48.
E-mail address: jbillen@vub.ac.be (J. Billen).

0021-9673/$ – see front matter © 2005 Elsevier B.V. All rights reserved.
doi:10.1016/j.chroma.2005.04.080

size. Assuming for the sake of simplicity a 10-fold reduction of the skeleton and domain size, and assuming that the plate heights would scale proportionally to the characteristic mass transfer distances as is the case for properly packed beds (minimal plate height is directly proportional to the diameter of the employed particles [8,9]), the above cited number of $N = 36{,}000$ plates could be achieved in a 10 times shorter column and in a 100 times shorter time, i.e., slightly over 1 min. Such a performance would be truly unprecedented and would for example have tremendous advantages in high-throughput applications or in the second dimension of 2D LC systems.

The above reasoning explains why the developers of monolithic columns are pushing towards the synthesis of columns with ever smaller domain sizes [6]. These attempts have up to now however been rather disappointing [2,6]. Comparing the domain size reduced plate heights of monoliths with a similar porosity always turned out in favour of the large domain monoliths, i.e., the produced small domain monoliths do not yield the same linear reduction of the plate heights as generally observed in packed bed columns.

Although there is an ongoing debate on which characteristic dimension should be selected to properly reduce the plate heights of silica monoliths [9], the fact that the domain size reduced plate heights of small domain monoliths are nearly always larger than those of large domain monoliths [2] is an irrefutable indication that small domain monoliths are more heterogeneous than their large domain counterparts. To understand this, it is first important to note that, at least on the macroscopic level, silica monoliths with a different scale but with a similar porosity can be considered to be self-similar. Self-similar structures are structures which can be made to perfectly overlap in a thought experiment by only varying their scale. As a consequence, structures can only be self-similar if they have the same ratio between the characteristic dimensions describing their structure. The two characteristic dimensions defining the structure of silica monoliths with a similar branch coordination number are the thickness and the length of the skeleton branches [10]. These are in turn related to the pore size and the domain size, usually defined as the sum of the pore size and the skeleton branch thickness [2], two other parameters generally used to describe the geometry of a monolith. Considering now for example the silica rod columns with a near identical external porosity of $\varepsilon = 0.61$–0.63 reported upon in [2], it is found that they have near constant pore to skeleton size ratios of respectively 2.43, 2.31, 2.30 and 2.31 whilst their domain size varies from $d_{dom} = 5.88\ \mu m$, over $d_{dom} = 3.85\ \mu m$ and $d_{dom} = 2.97\ \mu m$ to $d_{dom} = 2.27\ \mu m$. Since the domain size is the sum of the pore and skeleton size, it is obvious to find that the ratios of the domain to pore size and the domain to skeleton size are also nearly perfectly constant over the entire range of domain sizes. In fact they all lie between 1.70 and 1.77 and between 2.43 and 2.29, respectively. A similar domain size independence of the geometrical ratios is observed for the capillary silica monoliths reported on in [5], where columns MS-B and MS-D (both with an assumed external porosity of about 80%) for example have the same pore to skeleton size ratio of $d_{por}/d_s = 2.0$ and the same domain to skeleton size ratio $d_{dom}/d_s = 3.0$, despite of a significant difference in domain size ($d_{dom} = 4.2\ \mu m$ and $d_{dom} = 3\ \mu m$, respectively).

As explained by Giddings [11], it is one of the characteristic features of self-similar chromatographic support structures that they yield identical reduced plate height curves provided the reduction is based on one of the characteristic dimensions expressing the self-similarity of the structure. The reason for this perfect reducibility is that the band broadening in any chromatographic system is always determined by the same set of differential mass and impulse balances and boundary condition equations [12]. Making these equations dimensionless by dividing the spatial coordinates by one of the reference lengths, the ensuing equations only depend on a number of dimensionless parameters, the two most important of them being the Reynolds number (*Re*) and the Schmidt number (*Sc*). Both parameters furthermore always appear as their product, which is nothing else but the Peclet number (*Pe*) or the reduced velocity ν ($Pe = \nu = Re{\cdot}Sc$). Other parameters appearing in the dimensionless equations are the ratio of the stationary and the mobile zone diffusion coefficient (D_{sz}/D_{mol}) and a number of geometric ratios. In the case of self-similar packings, these geometric ratios are conditionally the same, implying that if the dimensionless mass and impulse balance equations are solved for two members of the same group of self-similar structures and for the same ν, the obtained solution for the passage of the eluting bands at a given dimensionless axial distance will be the same. The (dimensionless) second order moment (σ'^2) of these peaks, as well as the dimensionless plate height *h*, which is nothing else but the dimensionless axial gradient of σ'^2 ($h = \partial\sigma'^2/\partial x'$), will hence also be identical.

Returning now to the above mentioned observation that monoliths with similar d_{por}/d_{dom} and d_s/d_{dom}-ratio and porosity yield reduced plate height curves which tend to increase if the scale of their unit building block (i.e., the domain size) becomes smaller, it can only be concluded that these structures are not as self-similar as their near-identical average d_{por}/d_{dom} and d_s/d_{dom}-ratios would make one to believe. Since the ratios of the averaged characteristic dimensions suggest perfect self-similarity, the lack of agreement must be related to differences in the variance around these averages, bringing in the argument on the differences in pore network homogeneity, as has for example already been remarked in [2,6,9].

In the present study, it is assumed that this increased heterogeneity is caused by the existence of a domain size-independent lower limit on the variance of the size of the individual skeleton branches and through pores. It is assumed that this variance does not scale down in proportion to the characteristic dimensions of the packing, but instead displays a non-zero lower limit, brought about by local differences in the spinodal decomposition process, and impossible to surpass by shrinking the scale of the packing. Studying SEM pictures of silica monolith columns, it seems currently impossible to produce silica monoliths with skeleton

branches having a thickness and position variance smaller than a few tenths of a micrometer. On a large domain system ($d_{dom} > 10\ \mu m$), a size and position variability of this order only has a negligible influence on the packing homogeneity, but on a small domain system, the same size variance can be expected to have a detrimental effect on the structural homogeneity.

A similar non-zero lower limit variance effect can also be expected to eventually limit the performance of lithographically etched COMOSS [13,14] or porous pillar array columns [15,16], because even the most advanced current etching processes do not offer a perfect pillar size and position accuracy. The same effect can probably also be used to explain the apparent difficulties in preparing 1 or 2 μm particle packed bed columns yielding the same small reduced plate heights as a well-packed 10 μm particle bed column, although here packing efficiency problems also certainly come into play. If a particle synthesis process is used wherein the diameter of the particles can be controlled to within ±0.1 μm, this gives a size variability of 2% for $d_c = 10\ \mu m$ particles but already corresponds to a variability of 20% for $d_c = 1\ \mu m$ particles. Plate height increases caused by the existence of a lower limit size variance barrier can also be expected to influence the down-scaling of the packed bed columns used in CEC separations, since in this case the obtained plate heights are also still largely determined by packing heterogeneities [17,18].

Obviously, it might very well be that in practice this lower limit size variance barrier does not show up as a sharply delimited value but rather manifests itself over a broad transition range, depending on the synthesis process and the domain size. The present work should therefore be considered more as a "what if?"-study and an attempt to visualize the difficulties one could run into if attempting to further reduce the domain size of monoliths without finding a solution to reduce the size variances. To answer this "what if?"-question, a computational study has been conducted wherein a series of apparently self-similar structures (i.e., with near equal averaged size ratios) with varying domain size is subjected to a fixed, domain size-independent particle size and position variance. To isolate this size variability effect, nonporous structures are considered, as it is generally accepted that the packing heterogeneity mainly influences the *A*-term band broadening and does not influence the stationary zone diffusion and adsorption effects. For a qualitative description of the effect under study, it is also not needed to consider 3D systems. Certainly some typical 3D shape effects will be missed out by resorting to a 2D lay-out, but since the band broadening in each chromatographic process can be reduced to a problem of a series-parallel connection of different velocity zones [14], the general qualitative result of the present 2D study can be expected to hold independently of the dimension of the problem. Studying 2D systems has the advantage that they yield a more direct visual insight and allow for a more simple determination of the size variability parameters. In addition, the 2D approach requires only a fraction of the computational time needed for a 3D system.

2. Considered geometries and numerical methods

As the starting point for the present study, five perfectly ordered 2D cylinder arrays (cf. the grey coloured cylinder arrays in Fig. 1) with a different domain size but with the same external porosity (i.e., $\varepsilon = 0.6$) have been established. The arrays were drawn using the commercial CAD-software package Gambit® accompanying the Fluent® solver used to calculate the velocity fields and the tracer dispersion, as discussed below. The arrays were constructed by first drawing an equilateral triangular grid and by subsequently putting a cylinder on each grid point. As can be noted from Fig. 1A, the side of the equilateral triangle unit cell of this grid is the obvious measure for the domain size, for it corresponds to the sum of the cylinder diameter and the pore neck size, which is the now generally accepted definition [2] of the domain size in the monolithic column field. Making a few simple geometrical calculations, it can easily be verified that the adopted design rules lead to the following fixed ratio between the domain and the cylinder size:

$$\frac{d_{dom}}{d_c} = \frac{1}{2}\sqrt{\frac{2\pi}{\sqrt{3}(1-\varepsilon)}} \quad (1)$$

The value of this ratio is independent of the geometrical scale, and only depends on the value of the external porosity. Putting $\varepsilon = 0.6$ in Eq. (1), it can easily be verified that the equilateral triangular staggering always yields an external porosity of $\varepsilon = 0.6$ provided the cylinder diameter is exactly 1.5057 times smaller than the domain size (see ordered d_c- and d_{dom}-data in Table 1). This rule was applied to all considered arrays.

All flow domains consisted of 126 particles and were 6 particles wide by 21 particles long. The reader should note that, although the flow domains in Fig. 1 was rescaled to the same domain size, the simulations were carried out on flow domains corresponding to the nominal domain size. For example, the length and the width of the flow domain in the $d_{dom} = 6\ \mu m$-case were exactly six times larger than in the $d_{dom} = 1\ \mu m$-case (see Table 1 for all employed d_c- and d_{dom}-values). The representation in the constant domain size format adopted in Fig. 1 has been preferred over the actually used constant cylinder size format because it yields a more compact representation. It also immediately shows that the established ordered arrays are perfectly self-similar, i.e., they perfectly overlap when brought to the same scale.

In a second step, a series of five heterogeneous arrays (cf. black coloured cylinder arrays in Fig. 1) has been constructed by subjecting the position and the diameter of the individual cylinders of the ordered arrays to a random variation, using the evenly distributed random number generator of MS® Excell to define the new position and diameter of the individual cylinders. The absolute value of the variance on the centre position and the diameter of each cylinder was identical in all different domain size cases. In all cases, the maximal displacement of the cylinder centre was plus or minus 0.302 μm in both the *x*-direction and *y*-direction. The

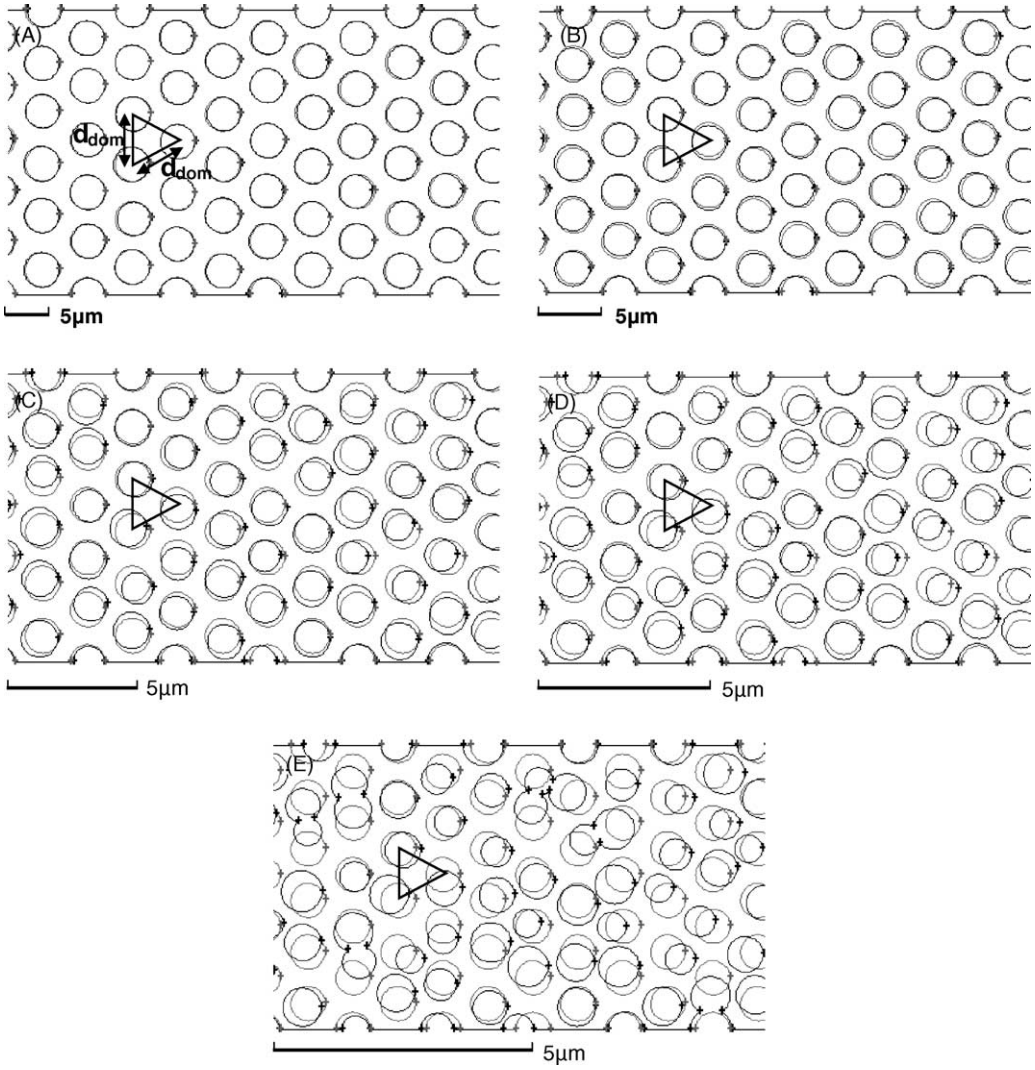

Fig. 1. Overlay plot of the considered 2D cylinder arrays (grey circles: perfectly ordered arrays; black circles: heterogeneous arrays) scaled to the same domain size. The equilateral triangular starting grid used to calculate the position of the cylinders in the ordered array cases is represented as well. Five different domain sizes have been considered: d_{dom} = 6 μm (A), d_{dom} = 4 μm (B), d_{dom} = 2 μm (C), d_{dom} = 1.5 μm (D), d_{dom} = 1 μm (E). The absolute variance on the position and the size of the individual cylinders is identical in all four cases (see text for more details).

random number generator randomly picked any of the possible values lying between the two extreme values with an equal probability. The diameter of the cylinders was in all domain size cases varied in an interval of 0.133 μm around the mean particle diameter. Introducing the heterogeneity in this way, it is ensured that the average domain size of each heterogeneous array will still be very close to the domain size of its corresponding ordered array and that the size and position variances are independent of the domain size.

Table 1
Domain, cylinder diameter and pore size values for the five different considered domain sizes

Domain size (μm)	Ordered arrays		Heterogeneous arrays		
	d_c (μm)	d_{por} (μm)	d_c ($\pm\sigma$) (μm)	d_{por} ($\pm\sigma$) (μm)	d_{dom} ($\pm\sigma$) (μm)
1	0.664	0.336	0.662 (±0.078)	0.361 (±0.211)	1.023 (±0.225)
1.5	0.996	0.504	0.994 (±0.078)	0.508 (±0.208)	1.502 (±0.222)
2	1.328	0.672	1.326 (±0.078)	0.674 (±0.217)	2.000 (±0.231)
4	2.657	1.344	2.654 (±0.078)	1.330 (±0.212)	3.984 (±0.226)
6	3.985	2.015	3.982 (±0.078)	2.008 (±0.206)	5.990 (±0.220)

The values given for the heterogeneous arrays are the average values calculated from the measured size distributions. The numbers between brackets are the standard deviations.

The numerical methods used to compute the flow field and the species dispersion, as well as the methods employed to calculate the plate height values from the recorded peak profiles are fully identical to those described in previous papers of our group [10,15,19,20] and are therefore not recaptured here. We will suffice by remarking that a commercial Computational Fluid Dynamics solver has been used (Fluent® 6.1.22, Fluent NV, Belgium) and that the accuracy of all presented calculations has been checked by varying the time step and the grid size.

To quantify the degree of packing heterogeneity of the different systems, distributions of the pore neck size (measured as the shortest distance between two neighbouring cylinders) and the cylinder diameter have been established. For the pore size distribution, 100 different shortest distance lines were drawn between two adjacent cylinders in random directions on jpg-file reproductions of the flow domains in Adobe Photoshop®. The lengths of the individual lines were subsequently determined using Imaq Vision Builder 5.0 software, directly providing the desired length distribution in an output file. In this way, the pore sizes are determined in a manner which is fully similar as to one would do when analysing a SEM picture of a real monolithic column. The distributions of the (exactly known) cylinder diameters could be established directly from the MS® Excell file used to generate them.

3. Results and discussions

A comparison of the grey and black coloured cylinder arrays in Fig. 1 directly allows to appreciate the strong increase in packing heterogeneity which follows upon a decrease of

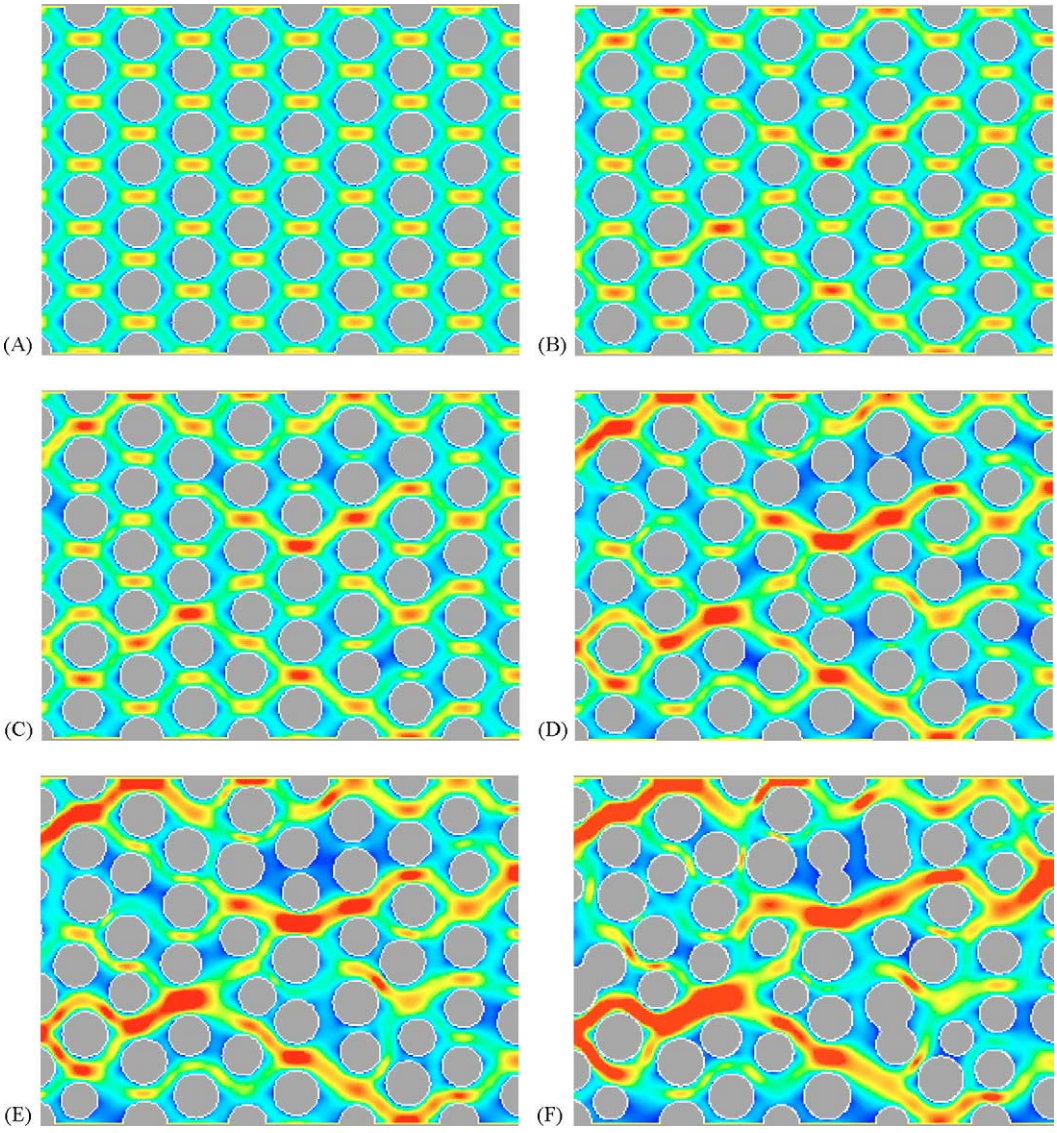

Fig. 2. Computed velocity fields in a perfectly ordered array (A) and in the five differently sized heterogeneous arrays (B–F). All cases have the same mean linear velocity. The colour scaling is proportional to the local u/u_{mean}-value, with u_{mean} defined as the largest local velocity encountered in the given domain (see text for colour details).

the domain size in the presence of a domain size independent lower limit on the cylinder size and position variance. The increased heterogeneity of the small domain structures is also clearly reflected in the calculated pore and cylinder size standard deviation values (Table 1). Whereas in absolute values these standard deviations are nearly perfectly identical in all five considered domain size cases (as could be expected from the rules used to establish the heterogeneous arrays), in relative terms, this standard deviation goes from a relatively small 1.96% (for the cylinder size) and 10.26% (for the pore size) in the 6 μm domain case to respectively 11.78% and 58.45% in the 1 μm domain case. Table 1 also shows an excellent agreement between the domain sizes of the perfectly ordered arrays and those of the heterogeneous arrays. Since the perfectly ordered arrays are perfectly self-similar, the heterogeneous arrays could, if the qualification would be based on the average characteristic dimensions (as is usually done), hence also be considered to be self-similar.

The velocity fields for the different heterogeneous arrays are however not self-similar at all (Fig. 2). To emphasize the differences between the different scale-structures, the computed velocity magnitude fields have been normalized to the mean local velocity magnitude (which was anyway identical in all the represented cases) and the colour scale was fixed between $u/u_{mean} = 0$ and $u/u_{mean} = 4$. In this way, the zones with the largest velocities are marked red and yellow (roughly $u > 3u_{mean}$), whereas the zones with the smallest velocities are marked blue (roughly $u < u_{mean}/5$). Going from Fig. 2A–F, it can readily be noted that, whereas all flow through pores in the perfectly ordered and the largest domain heterogeneous array (Fig. 2A and B) have a nearly identical status and are permeated with the same intensity, the flow through the heterogeneous arrays with the smallest domain size (Fig. 2D–F) is divided in only a few preferential flow paths where the velocity is much larger than in the remainder of the packing. The presence of these preferential flow paths in turn obviously has a dramatic impact on the band broadening, as can clearly be assessed from Fig. 3.

Quantifying the band broadening in all different considered ordered and heterogeneous array cases by calculating the corresponding plate heights over a range of different velocities yields the series of van Deemter curves shown in Fig. 4. For the ordered array cases (dashed curves), the normal behaviour of self-similar systems is noted, i.e., the minimal plate heights decrease linearly with the domain or cylinder size. The difference with the van Deemter curves for the heterogeneous arrays (full lines) is striking. Not only do the curves lie significantly higher, the lowest plate height curve no longer corresponds to the packing with the smallest domain size but to one with an intermediate value, i.e., with $d_{dom} = 2$ μm. This result implies that any manufacturing method producing a residual, domain-size independent minimal size and position variance will be marked by the existence of a lower plate height limit which cannot be passed by decreasing the domain size of the packing structure.

In Fig. 5, the van Deemter curves shown in Fig. 4 are reconsidered in dimensionless coordinates. Whereas the ordered array cases all reduce to the same curve (dashed line), in agreement with their perfect self-similarity, the heterogeneous array cases clearly deviate from this "perfect standard" curve, although they all have the same ratios between their average characteristic dimensions. The cases with the smallest domain size, i.e., the cases with the largest heterogeneity, clearly yield the largest deviation. The use of d_{dom}-reduced

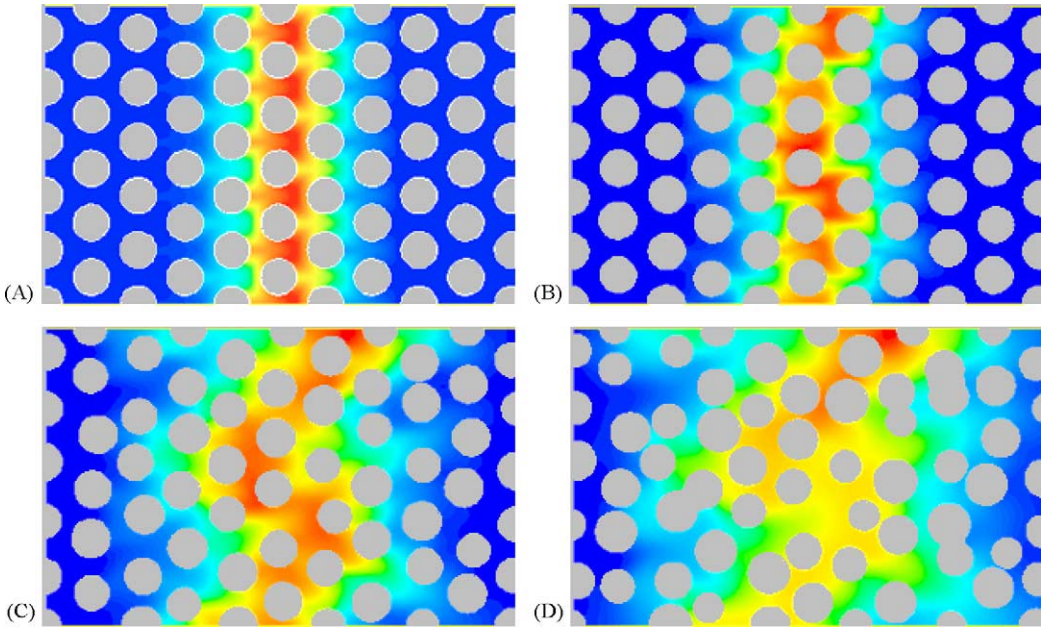

Fig. 3. Plot of a species plug shortly after its introduction at the inlet of the flow domain for the perfectly ordered array case (A) and for three of the different heterogeneous cylinder arrays: $d_{dom} = 6$ μm (B), $d_{dom} = 2$ μm (C), $d_{dom} = 1$ μm (D).

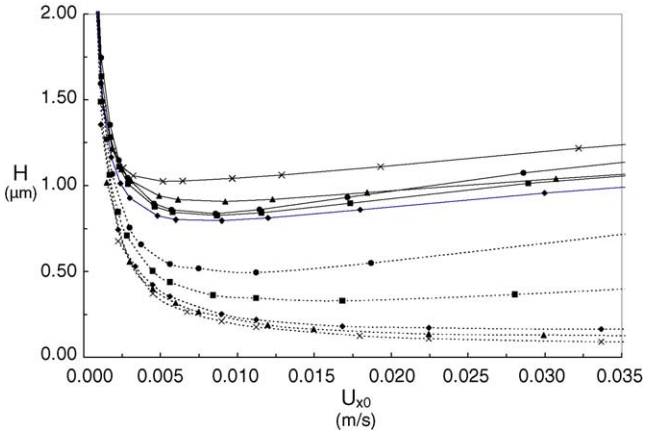

Fig. 4. van Deemter plots of the plate heights calculated for the five considered domain sizes (d_{dom} = 6 μm (●), 4 μm (□), 2 μm (♦), 1.5 μm (▲), 1 μm (×)) in the ordered (dashed lines) and the heterogeneous array cases (full lines).

plate heights hence yields a very sensitive means to assess the degree of heterogeneity of a given packing. The largest domain size case, wherein the presence of size variance is nearly invisible to the eye, also already yields a deviation from the perfectly ordered array curve.

It should be noted that the plate height values in Figs. 4 and 5 only relate to the *A*- and *B*-term band broadening, and that in real porous columns the small domain monolith heterogeneity effect will be tempered (but not eliminated!) by the band broadening contributions stemming from the stationary zone mass transfer resistance. It can, however, be inferred from the additive effect of the different band broadening contributions [11] that the main conclusion of Figs. 4 and 5 also holds for porous structures.

Another remark to be made, is that the present results are for a system with an external porosity of $\varepsilon = 0.6$, corresponding roughly to the external porosity in commercial wide-bore silica monolith columns. It is obvious that, if the same fixed minimal skeleton size and position variance would prevail, packings with a smaller porosity (i.e., $\varepsilon < 0.6$) will

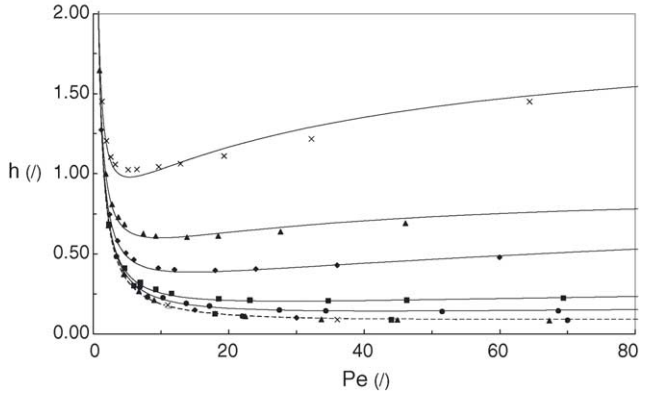

Fig. 5. Reduced plate height curves based on d_{dom} (same symbols as in Fig. 4. The full and dashed lines are obtained by fitting Eq. (2) to the computed plate height data.

Table 2
Knox parameters obtained after fitting the domain size reduced plate height data shown in Fig. 5 to Eq. (2)

Domain size (μm)	*A* (–)	*B* (–)	*C* (–)
1	0.381	1.333	0
1.5	0.196	1.388	0
2	0.119	1.396	0
4	0.050	1.466	0
6	0.031	1.530	2.04×10^{-6}
Uniform arrays	0.015	1.505	$7.80 \times 10e^{-5}$

display an even stronger *A*-term band broadening than in the present case, whereas packings with a larger porosity (say $\varepsilon = 0.8$–0.9) would be less affected.

Fitting the reduced plate height curves shown in Fig. 5 with the frequently used empirical Knox-equation:

$$h = Av^{1/3} + \frac{B}{v} + Cv \tag{2}$$

it is found that the increased heterogeneity of the small domain structures is mainly reflected in the *A*-term band broadening (cf. Table 2), as could be expected from the physical meaning of the latter [9]. Going from the perfectly ordered array case, where $A = 0.015$, to the maximally heterogeneous case with $d_{dom} = 1$ μm, where $A = 0.38$, a near 25-fold increase in the *A*-term band broadening is observed. The *B*-term constant values vary much less, and the *C*-term constant values are so small compared to the *A*-term contribution that in most cases this value had to be fixed to zero in order to prevent the fitting algorithm to produce physically unfeasible negative *C*-values. The poor fitting for the smallest domain size cases reflects the fact that the $n = 1/3$ Knox-equation only has empirical grounds. Fittings with free *n* yielded much better fittings, but since the exponent *n* varied in a rather random manner from case to case we preferred to stick to the $n = 1/3$ model.

Fig. 6 shows a plot of the *A*-term constant and the relative domain size variance (σ^2_{dom}/d^2_{dom}) as a function of the domain size for the different heterogeneous array cases. Both lines run nearly parallel, indicating a tight link between both quantities. In both cases, a vertical asymptote is reached for a domain size just below $d_{dom} = 1$ μm. It is thought that making this type of plots, i.e., plotting either *A* versus d_{dom} or σ^2_{dom}/d^2_{dom}

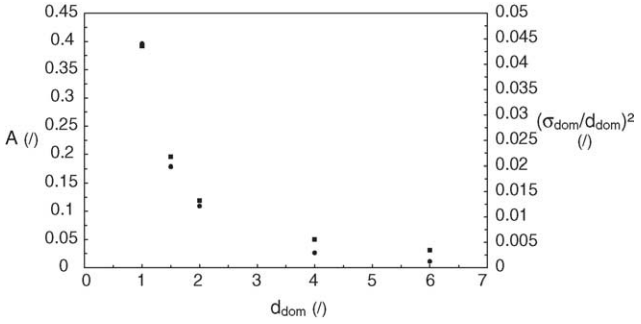

Fig. 6. Dependency of the *A*-term constant (■) and $(\sigma_{dom}/d_{dom})^2$ (●) on the domain size d_{dom}.

versus d_{dom} for a series of columns produced with a similar method but with different domain size, could be very useful to determine the presence of a lower limit size variance barrier. If A and σ^2_{dom}/d^2_{dom} would remain more or less constant, this would indicate that the size variance decreases together with the domain size, allowing to conclude that the employed synthesis method does not have a fixed variance size barrier. On the other hand, if A and σ^2_{dom}/d^2_{dom} would display a sharp increase, this would then be a clear indication of the existence of a lower limit size variance barrier. It can however be expected that the σ^2_{dom}/d^2_{dom}-values will reach a maximum around $\sigma^2_{dom}/d^2_{dom} = 1$, since this represents the case where the standard deviation is as large as the domain size. From the tight link between A and σ^2_{dom}/d^2_{dom}, it suffices of course to measure only one of both parameters. The determination of A, requiring only a fit of the van Deemter data with Eq. (2) obviously is much easier than the determination of σ^2_{dom} which requires the use of some optical scanning technique in combination with a geometrical reconstruction routine. The latter method can however be assumed to be more accurate than the A-term constant fitting method.

4. Conclusions

Given that the pore and skeleton size variance in monolithic columns is directly related to the stochastic nature of the spinodal decomposition process, it is not unreasonable to assume that this variance will not scale down in proportion with the domain size, but will, from a given domain size on, remain at a given non-zero level, independently of the domain size. Computing the A-term band broadening in a series of apparently self-similar structures (same mean geometric ratios and same porosity) with decreasing scale, the present computational study shows that the existence of such a minimal size variance barrier will lead to a lower limit van Deemter curve and that any attempt to pass this lower limit by further decreasing the domain and skeleton size without being able to co-reduce the size variance will inevitably result in an increase instead of a further decrease of the plate heights. Although the existence of such a lower limit on the size variance has not been investigated yet, the concept can be used to understand the major difficulties encountered when trying to synthesize high performance small domain monoliths.

The present results indicate that the key to obtaining high quality small domain size monoliths (say with $1\ \mu m < d_{dom} < 3\ \mu m$) will lie in the ability to reduce the standard deviation on the size and the position of the skeleton branches to below 0.1 μm or even 0.05 μm and that extensive studies of the relationship between the exact process conditions and the structural variances will become absolutely critical in the next development stages. Column preparation reports should therefore not only mention average skeleton and pore sizes, but should also include variance data. Conducting systematic studies wherein the size variability is quantified as a function of the experimental conditions (duration and intensity of the reagent mixing, temperature control, . . .) will undoubtedly give clues on how the current monolith manufacturing methods could be improved. For this purpose, microscopic visualization methods, like for example the laser scanning confocal microscopy (LSCM) method proposed in [21], will become indispensable research tools. Introducing more vigorous mixing methods such as ultrasonic [22] or chaotic advection [23] mixing in microfluidic channels producing the smallest possible mixing eddies could be one of the possible solutions to improve the size variability of small domain monoliths.

5. Nomenclature

A, B, C	Knox equation constants (–)
d_c	cylinder diameter (m)
d_{dom}	domain size, see Fig. 1 (m)
d_{por}	pore size (m)
d_{ref}	general characteristic dimension (m)
d_s	skeleton diameter (m)
D_{mol}	molecular diffusion coefficient in mobile zone (m^2/s)
D_{sz}	molecular diffusion coefficient in stationary zone (m^2/s)
h	reduced theoretical plate height ($h = H/d_{ref}$)
H	height equivalent of a theoretical plate (m)
L	length op the separation column (m)
N	number of plates
Pe	Peclet number
Re	Reynolds number, $Re = u \cdot d_{ref}/D_{mol}$ (–)
Sc	Schmidt number, $Sc = \eta/D_{mol}$ (–)
u	local interstitial mobile phase velocity (m/s)
u_0	mean velocity of permeating, but non-retained solute (m/s)
u_{mean}	mean interstitial mobile phase velocity (m/s)
u_{opt}	optimal mean interstitial mobile phase velocity (m/s)
x':	axial distance in the column divided by reference dimension (–)

Greek symbols

ε	external column porosity (–)
η	kinematic viscosity (m^2/s)
ν	reduced fluid velocity, based on u_0 ($=u_0 \cdot d_{dom}/D_m$)
σ'^2	dimensionless second order moment (–)
σ_{por}	standard deviation on the pore size (m)

Acknowledgements

The authors gratefully acknowledge a research grant (FWO KNO 81/00) from the Fund for Scientific Research-Flanders (Belgium). P.G. is supported through a specializa-

tion grant from the Instituut voor Wetenschap en Technologie (IWT) of the Flanders Region (grant nr. SB/11419). We also thank Sebastiaan Eeltink and Peter Schoenmakers from the Polymer Analysis group of the University of Amsterdam for the stimulating discussions.

References

[1] H. Minakuchi, K. Nakanishi, N. Soga, N. Ishizuka, N. Tanaka, Anal. Chem. 68 (1996) 3498.
[2] H. Minakuchi, K. Nakanishi, N. Soga, N. Ishizuka, N. Tanaka, J. Chromatogr. A 797 (1998) 121.
[3] J.E. Mac Nair, K.D. Patel, J.W. Jorgenson, Anal. Chem. 71 (1999) 700.
[4] A.D. Jerkovich, J.S. Mellors, J.W. Jorgenson, LC–GC Eur. 16 (2003) 20.
[5] M. Motokawa, H. Kobayashi, N. Ishizuka, H. Minakuchi, K. Nakanishi, H. Jinnai, K. Hosoya, T. Ikegami, N. Tanaka, J. Chromatogr. A 961 (2002) 53.
[6] N. Tanaka, H. Kobayashi, N. Ishizuka, H. Minakuchi, K. Nakanishi, K. Hosoya, T. Ikegami, J. Chromatogr. A 965 (2002) 35.
[7] K. Cabrera, D. Lubda, A. Kraus, H. Minakuchi, K. Nakanishi, Lecture L-0407 at 28th International Symposium and Exhibit on High Performance Liquid Phase Separations and Related Techniques, Philadelphia, USA, 2004.
[8] H. Poppe, J. Chromatogr. A 778 (1997) 3.
[9] J.H. Knox, J. Chromatogr. A 960 (2002) 7.
[10] N. Vervoort, P. Gzil, G.V. Baron, G. Desmet, J. Chromatogr. A 1030 (2004) 177.
[11] J.C. Giddings, Dynamics of Chromatography-Part I, Marcel Dekker Inc, New York, 1965.
[12] G. Guiochon, S.G. Shirazi, A.M. Katti, Fundamentals of preparative and nonlinear chromatography, Academic Press, London, 1994.
[13] B. He, F. Regnier, J. Pharm. Biomed. Anal. 17 (1998) 925.
[14] B.E. Slentz, N.A. Penner, E. Lugowska, F. Regnier, Electrophoresis 22 (2001) 3736.
[15] P. Gzil, N. Vervoort, G.V. Baron, G. Desmet, Anal. Chem. 75 (2003) 6244.
[16] P. Gzil, J. De Smet, N. Vervoort, H. Verelst, G.V. Baron, G. Desmet, J. Chromatogr. A 1030 (2004) 53.
[17] E. Wen, R. Asiaie, Cs. Horvath, J. Chromatogr. A 855 (1999) 349.
[18] K. Walhagen, K.K. Unger, M.T.W. Hearn, J. Chromatogr. A 887 (2000) 165.
[19] P. Gzil, G.V. Baron, G. Desmet, J. Chromatogr. A 991 (2003) 169.
[20] P. Gzil, N. Vervoort, G.V. Baron, G. Desmet, J. Sep. Sci. 27 (2004) 887.
[21] H. Jinnai, K. Nakanishi, Y. Nishikawa, J. Yamanaka, T. Hashimoto, Langmuir 17 (2001) 619.
[22] G.G. Yaralioglu, I.O. Wygant, T.C. Marentis, B.T. Khuri-Yakub, Anal. Chem. 76 (2004) 3694.
[23] H. Aref, Phys. Fluids 14 (2002) 1315.